Determinable and non-determinable parameters of galvanic distortion in magnetotellurics

H. M. Bibby,[1] T. G. Caldwell[1,2] and C. Brown[2]

[1]*Institute of Geological and Nuclear Sciences,* PO Box 30368, *Lower Hutt, New Zealand,* 6315. *E-mail: h.bibby@gns.cri.nz*
[2]*National University of Ireland, Department of Earth and Ocean Sciences, Galway, Ireland*

SUMMARY

Galvanic distortion has long been recognized as an obstacle in the interpretation of magnetotelluric (MT) data. One fundamental problem for distortion removal is that the equations that describe the effects of galvanic distortion on the impedance tensor are underdetermined. We have previously shown that an explicit solution for four of the parameters of the regional (undistorted) impedance tensor can be resolved without any assumptions. These determinable parameters are the components of a tensor (the phase tensor) representing the phase information contained in the impedance. The coordinate invariants of the phase tensor provide a simple and objective guide to the dimensionality of the regional impedance tensor at each measured frequency. Where the regional structure is 2-D, one of the principal axes of the phase tensor will be aligned parallel to the strike of the regional conductivity. The distortion tensor and the parameters of the regional impedance tensor that represent the amplitude information cannot be determined without assumptions. Where the phase tensor shows the regional impedance tensor to be 1-D, the distortion tensor and the regional impedance can be determined to within a single multiplicative constant. Where a 2-D regional structure is indicated, two assumptions are necessary to determine the regional impedance tensor but the solution is not unique, and any choice of assumptions could be made with equal validity. For 3-D structures, the phase tensor provides the direction of greatest inductive response, which is the closest equivalent of a strike direction. In this case four constraints are required for a solution. In practice, a MT sounding may contain sections that display different characteristic dimension and the distortion tensor can be determined from the section of the sounding with the lowest characteristic dimension. The greatest amount of information is determined from a 1-D section. The use of the information contained in the phase tensor overcomes some of the shortcomings of traditional distortion analysis. Illustrating the tensors using an elliptical representation aids the interpretation of the tensor data involved in this analysis.

Key words: electromagnetic methods, galvanic distortion, geo-electrical strike, magnetotellurics, phase tensor, regional conductivity.

INTRODUCTION

Galvanic distortion is often observed in magnetotelluric (MT) measurements. Galvanic distortion can be regarded as the superposition of the (frequency independent) signatures of localized, near-surface (3-D) heterogeneities on the (frequency dependent) signature of the larger-scale regional structure. Such distortion can mask the properties of the larger-scale structure that is the usual target of the MT surveys. The primary aim of distortion analysis is to eliminate the influence of the near-surface heterogeneities from the measured MT impedance tensor and hence determine the impedance tensor that represents the regional structure alone. Ideally this would be done without having to make any assumption regarding the nature of the regional structure.

There have been a number of different approaches to deriving a solution for the regional (undistorted) impedance tensor. The most common techniques used for distortion removal are the decomposition method of Groom & Bailey (1989, 1991), hereafter referred to as G&B, and the related technique of Smith (1995). In both these methods distortion analysis is also used as a means of determining an appropriate strike of the regional structure, assuming that structure to be 2-D (e.g. McNeice & Jones 2001). In this form, G&B analysis has almost taken on the role of pre-conditioning MT survey data prior to 2-D modelling. The basis of these approaches is not intuitively obvious and their physical basis remains controversial. An alternative approach to the problem is that of Bahr (1988, 1991), which is based on the analysis of the phase and is aimed primarily at determining the dimension of the regional (undistorted) MT

data, and estimating the strike direction. Good summaries of these and other approaches can be found in McNeice & Jones (2001) and Ritter (1996), for example. A more general approach was made by Weaver *et al.* (2000) who used a carefully selected set of invariants of the impedance tensor to deduce the inherent regional dimensionality and to identify the presence of distortion. These invariants can be linked to the properties of the phase tensor (Weaver *et al.* 2003).

In analysing the problem of distortion removal, Smith (1995) pointed out that the mathematical description of the full distortion problem involves finding a solution for a set of equations that is underdetermined and that a solution is not possible without assumptions. It should be of concern, however, that the set of assumptions made by both G&B and Smith (1995) reduces the underdetermined set of equations to an over-determined set, which is subsequently solved using a least squares approach. This reduction of the problem from an underdetermined to an over-determined set of equations suggests that, for the general case, too many constraints have been applied. Indeed we show below that one determinable parameter of the general problem is inadvertently assumed to be zero in these approaches.

The key step in understanding the limitations of distortion removal is in the recognition that the set of underdetermined equations of distortion has a partial solution, which can be determined without any assumption. This partial solution for the regional impedance is represented by the four components of a tensor: the phase tensor (Caldwell *et al.* 2004 from herein referred to as CBB). Using the phase tensor it is possible to determine the characteristic dimension (or symmetry) of the regional impedance tensor and, for 2-D situations, the strike direction. Thus the problem of determining the strike direction can be separated from that of determining the distortion, as was shown by Bahr (1988, 1991) in his analysis of the phase. The assumption of 2-D regional structure tacitly assigns one of the determinable parameters to be identically zero, that parameter being the indicator of 3-D. The solution for the distortion tensor and the remaining components of the regional impedance tensor cannot be solved without assumptions. However, we show here that the information provided by the phase tensor on the dimension of the regional impedance tensor can be used as a guide to the subsequent analysis and allows the minimum number of assumptions to be made: one, two or four assumptions for 1-D, 2-D or 3-D, respectively. The nature of the assumptions and their significance are also illustrated.

GALVANIC DISTORTION OF THE ELECTRIC FIELD

The theory describing the galvanic distortion of MT measurements is now well established (e.g. Groom & Bahr 1992; Chave & Smith 1994) and is only briefly summarized here. Distortion is usually described in terms of the influence of small localized conductivity heterogeneities, which alter the direction and magnitude of the electric field at the measurement site. At periods (T) greater than some threshold value, T_c, inductive effects within these conductivity heterogeneities become negligible compared with the inductive response produced by the regional conductivity structure (e.g. Jiracek 1990). For periods greater than T_c, the effect of the heterogeneities on the electric field vector can be regarded as independent of period and, thus, the measured electric field, $\mathbf{E}$, can be represented as a linear function of the regional electric field $\mathbf{E_R}$ (the electric field that would be measured in the absence of the heterogeneities). With this

approximation, the measured electric field, $\mathbf{E}$, can be written as

$$\mathbf{E} = \mathbf{D}\,\mathbf{E_R}; \quad T > T_c, \tag{1}$$

where $\mathbf{D}$, the distortion tensor, is real and is independent of period (Groom & Bahr 1992; Chave & Smith 1994). The influence of the distortion is to change the magnitude and direction of the electric field but, as $\mathbf{D}$ is real, the phase relationships are preserved. In Cartesian coordinates $\mathbf{D}$ can be written as a 2×2 matrix:

$$\mathbf{D} = \begin{bmatrix} D_{11} & D_{12} \\ D_{21} & D_{22} \end{bmatrix}. \tag{2}$$

Although it is possible to also have distortion of the magnetic field (Groom & Bahr 1992; Singer 1992; Chave & Smith 1994), we will assume that no magnetic distortion is present so that the horizontal component of the measured magnetic field $\mathbf{H}$ is, to a good approximation, equal to the corresponding regional magnetic field $\mathbf{H_R}$.

The MT impedance tensor $\mathbf{Z}$ is defined by the relationship between the measured electric and magnetic fields

$$\mathbf{E} = \mathbf{Z}\,\mathbf{H}. \tag{3}$$

If no distortion is present the impedance tensor representing the regional structure $\mathbf{Z_R}$ is given by

$$\mathbf{E_R} = \mathbf{Z_R}\,\mathbf{H_R}. \tag{4}$$

Therefore, from 1 and 3

$$\mathbf{E} = \mathbf{D}\,\mathbf{E_R} = \mathbf{D}\,\mathbf{Z_R}\,\mathbf{H_R} = [\mathbf{D}\,\mathbf{Z_R}]\,\mathbf{H} \tag{5}$$

and the relationship between the regional and observed impedance tensors can be written

$$\mathbf{Z} = \mathbf{D}\,\mathbf{Z_R}. \tag{6}$$

This is the key equation of galvanic distortion. To eliminate the effects of distortion on measured MT data, it is necessary to determine $\mathbf{Z_R}$ from a given $\mathbf{Z}$. However, eq. (6) represents a set of eight equations in twelve unknowns (four components of $\mathbf{D}$ and eight components of $\mathbf{Z_R}$) so that the set of equations is underdetermined.

THE PHASE TENSOR

Despite the underdetermined nature of eq. (6) a partial solution is possible without any assumptions. This partial solution is represented most easily by the phase tensor of CBB. The key elements of the phase tensor derivation are given below.

By splitting the impedance tensors $\mathbf{Z}$ and $\mathbf{Z_R}$ into real ($\mathbf{X}$) and imaginary ($\mathbf{Y}$) parts

$$\mathbf{Z} = \mathbf{X} + i\,\mathbf{Y} \quad \text{and} \quad \mathbf{Z_R} = \mathbf{X_R} + i\,\mathbf{Y_R} \tag{7}$$

we can rewrite eq. (6) as two equations

$$\mathbf{X} = \mathbf{D}\,\mathbf{X_R}, \tag{8}$$

$$\mathbf{Y} = \mathbf{D}\,\mathbf{Y_R}. \tag{9}$$

We define a phase tensor $\mathbf{\Phi}$ as

$$\mathbf{\Phi} = \mathbf{X}^{-1}\,\mathbf{Y}, \tag{10}$$

where $\mathbf{X}^{-1}$ is the inverse of $\mathbf{X}$. From eqs (8) and (9),

$$\begin{aligned} \mathbf{\Phi} &= (\mathbf{D}\,\mathbf{X_R})^{-1}\,(\mathbf{D}\,\mathbf{Y_R}) \\ &= \mathbf{X_R}^{-1}\,\mathbf{D}^{-1}\,\mathbf{D}\,\mathbf{Y_R} = \mathbf{X_R}^{-1}\,\mathbf{Y_R} \\ &= \mathbf{\Phi_R}. \end{aligned} \tag{11}$$

Thus the measured and the regional phase tensors are identical and are independent of galvanic distortion. The phase tensor of the regional impedance, $\boldsymbol{\Phi_R}$, is thus a partial solution to the equations of distortion (6). The four components of the phase tensor, which are simple functions of the components of the measured impedance tensor, are in general, the only uniquely determinable portion of the regional impedance tensor. This partial solution of the distortion equations requires no assumption about the nature of the conductivity distribution or the forms of the distortion and regional impedance tensors. Indeed, the phase tensor provides information on the nature of the regional conductivity structure, as is shown below.

Expanding eq. (10) in terms of the components $\mathbf{X}$ and $\mathbf{Y}$, the phase tensor can be written

$$\boldsymbol{\Phi} = \begin{bmatrix} X_{22}Y_{11} - X_{12}Y_{21} & X_{22}Y_{12} - X_{12}Y_{22} \\ X_{11}Y_{21} - X_{21}Y_{11} & X_{11}Y_{22} - X_{21}Y_{12} \end{bmatrix} \Big/ \det(\mathbf{X})$$

$$= \begin{bmatrix} \Phi_{11} & \Phi_{12} \\ \Phi_{21} & \Phi_{22} \end{bmatrix}, \tag{12}$$

where $\det(\mathbf{X}) = X_{11}X_{22} - X_{21}X_{12}$.

The explicit expression for the phase tensor (eq. 12) allows the error estimates in $\mathbf{Z}$ to be propagated rigorously to all subsequent functions of the phase tensor.

Properties and visualization of the phase tensor

The properties of the phase tensor are best presented by the use of tensor invariants. There are three independent invariants for any 2-D, second rank tensor. We will represent the phase tensor in two related forms (CBB and Bibby 1986). From Bibby (1986) we write

$$\boldsymbol{\Phi} = \Pi_1 \begin{bmatrix} \cos 2\alpha_\Phi & \sin 2\alpha_\Phi \\ \sin 2\alpha_\Phi & -\cos 2\alpha_\Phi \end{bmatrix} + \Pi_2 \begin{bmatrix} \cos 2\beta_\Phi & \sin 2\beta_\Phi \\ -\sin 2\beta_\Phi & \cos 2\beta_\Phi \end{bmatrix}, \tag{13}$$

where Π_1, Π_2 and β_Φ are independent invariants, and α_Φ is dependent on the coordinate axes used. Angles α_Φ and β_Φ can be expressed in terms of the components of $\boldsymbol{\Phi}$ as

$$\tan 2\alpha_\Phi = (\Phi_{12} + \Phi_{21})/(\Phi_{11} - \Phi_{22})$$
$$\tan 2\beta_\Phi = (\Phi_{12} - \Phi_{21})/(\Phi_{11} + \Phi_{22}) \tag{14}$$

and similarly

$$\Pi_1 = \frac{1}{2}\left[(\Phi_{11} - \Phi_{22})^2 + (\Phi_{12} + \Phi_{21})^2\right]^{1/2}$$
$$\Pi_2 = \frac{1}{2}\left[(\Phi_{11} + \Phi_{22})^2 + (\Phi_{12} - \Phi_{21})^2\right]^{1/2}. \tag{15}$$

The phase tensor (and indeed any 2×2 real matrix) can be graphically represented as an ellipse the properties of which can be described by the parameters given above (Fig. 1 and Appendix). In particular, the semi-major and semi-minor axes of the ellipse are given by $\Phi_{max} = \Pi_2 + \Pi_1$ and $\Phi_{min} = \Pi_2 - \Pi_1$ and the orientation of the major axis is given by $\alpha_\Phi - \beta_\Phi$. The angle α_Φ defines the position of a reference axis relative to the coordinate axes and β_Φ defines the position of the principal axis of the ellipse relative to the reference axis. Rotating the coordinate axes will change the angle between the reference axis and the coordinate axes, but the shape and geographic position of the ellipse will be unchanged. This graphical representation (Fig. 1) provides an intuitively simple means of illustrating the properties of any of the tensors ($\mathbf{X}$, $\mathbf{Y}$, $\mathbf{D}$, $\boldsymbol{\Phi}$) used in MT analysis. Note that as the phase tensor is a function of the impedance tensor, the phase tensor invariants can be expressed as functions of the invariants of the impedance tensor as was demonstrated by Weaver *et al.* (2003).

Although there are only three independent invariants any combination of invariants will also be an invariant. In particular, the magnitudes of the principal axes of the phase tensor ellipse Φ_{max} and Φ_{min} (Fig. 1, Appendix) are invariants. For later dimensional analysis we also introduce the non-dimensional ratio $\lambda = \Pi_1/\Pi_2$.

Using these invariants, the phase tensor can be written in the alternative form (CBB)

$$\boldsymbol{\Phi} = \mathbf{R}^{\mathbf{T}}(\alpha_\Phi - \beta_\Phi)\begin{bmatrix} \Phi_{max} & 0 \\ 0 & \Phi_{min} \end{bmatrix}\mathbf{R}(\alpha_\Phi + \beta_\Phi), \tag{16}$$

where $\mathbf{R}$ is the rotation matrix
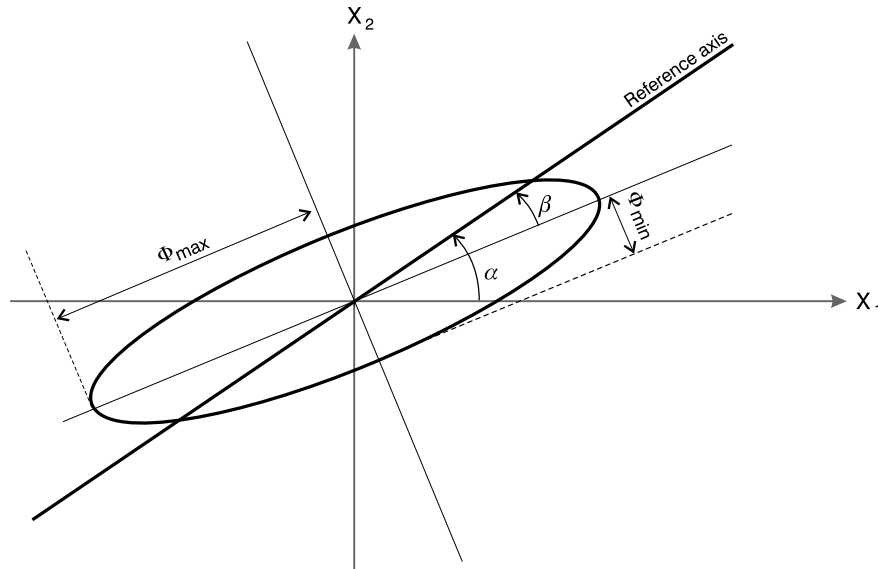
Figure 1. The graphical representation of a tensor as an ellipse (see Appendix). The semi-major and semi-minor axes of the ellipse are defined by the coordinate invariants Φ_{max} and Φ_{min}, respectively. The invariants (β, Φ_{max} and Φ_{min}) represent the intrinsic physical properties of the tensor that are not dependent on the reference frame.

$$\mathbf{R}(\theta) = \begin{bmatrix} \cos\theta & \sin\theta \\ -\sin\theta & \cos\theta \end{bmatrix} \tag{17}$$

and superscript T indicates the matrix transpose.

Phase tensor and dimensionality of the regional conductivity

1-D structure

If the regional structure is 1-D, the impedance $\mathbf{Z_R}$ will be independent of the coordinate axes and takes the antidiagonal form

$$\mathbf{Z_R} = \begin{bmatrix} 0 & Z_{1D} \\ -Z_{1D} & 0 \end{bmatrix}. \tag{18}$$

Thus from eq. (12) the phase tensor can be written

$$\mathbf{\Phi}_{1D} = (Y_{1D}/X_{1D})\,\mathbf{I}, \tag{19}$$

where $\mathbf{I}$ is the identity matrix, and $(Y_{1D}/X_{1D}) = \mathrm{Im}(Z_{1D})/\mathrm{Re}(Z_{1D})$ is the tangent of the (scalar) phase.

By comparison of eq. (19) with eq. (13), the necessary conditions for regional 1-D structure are

$$\Pi_1 = 0 \ (\text{or } \Phi_{\max} = \Phi_{\min}) \text{ and } \beta_\Phi = 0 \tag{20}$$

or equivalently, in terms of the components of $\mathbf{\Phi}$

$$\Phi_{12} = \Phi_{21} = 0 \text{ and } \Phi_{11} = \Phi_{22}. \tag{21}$$

In the graphical representation of the phase tensor as an ellipse (Fig. 1) the major and minor axes ($\Phi_{\max}$ and $\Phi_{\min}$) become equal and the ellipse reduces to a circle. Note that in this case the principal axes are undefined or equivalently, the coordinate dependent term α_Φ is undefined. This is equivalent to the observation that the strike is undefined in a 1-D situation (see discussion of 2-D below). The requirement for eq. (19) to be non-trivial is that the phase, $\tan^{-1}(Y_{1D}/X_{1D})$, is defined. In terms of the invariants this requires

$$(Y_{1D}/X_{1D}) = \Pi_2 \neq 0. $$

Hence the necessary conditions for 1-D (eq. 20) can be written in the dimensionless form

$$\lambda = \Pi_1/\Pi_2 = 0 \text{ and } \beta_\Phi = 0. \tag{22}$$

2-D structure

For an idealized 2-D structure, the impedance tensor is purely antidiagonal when the coordinate axes are rotated to be parallel (or perpendicular) to the conductivity strike. That is,

$$\mathbf{Z_R} = \mathbf{R}^{\mathrm{T}}(\psi) \begin{bmatrix} 0 & Z'_{12} \\ Z'_{21} & 0 \end{bmatrix} \mathbf{R}(\psi), \tag{23}$$

where ψ is the strike direction with respect to the observational coordinate system. (We denote parameters defined in coordinates aligned with the strike direction by primes.) Writing eq. (23) in its real and imaginary parts, using $\mathbf{Z}' = \mathbf{X}' + i\,\mathbf{Y}'$ the phase tensor can

be written as

$$\mathbf{\Phi}_{2D} = \{\mathbf{R}^{\mathrm{T}}(\psi) \begin{bmatrix} 0 & X'_{12} \\ X'_{21} & 0 \end{bmatrix} \mathbf{R}(\psi)\}^{-1}\, \mathbf{R}^{\mathrm{T}}(\psi) \begin{bmatrix} 0 & Y'_{12} \\ Y'_{21} & 0 \end{bmatrix} \mathbf{R}(\psi)$$

$$= \mathbf{R}^{\mathrm{T}}(\psi) \begin{bmatrix} Y'_{21}/X'_{21} & 0 \\ 0 & Y'_{12}/X'_{12} \end{bmatrix} \mathbf{R}(\psi). \tag{24}$$

Comparing eqs (24) and (16), the necessary condition for 2-D is simply $\beta_\Phi = 0$. When this applies, the strike direction relative to the measurement axes is given by $\psi = \alpha_\Phi$ and the principal components become $Y'_{21}/X'_{21} = \Phi_{\max}$ and $Y'_{12}/X'_{12} = \Phi_{\min}$. Note that when distortion is present, the strike direction must be determined from the phases, as has been previously noted by other authors (e.g. Bahr 1988; Berdichevsky 1999). The effect of distortion on the measured impedance tensor $\mathbf{Z}$ is to modify the amplitudes and thus the strike information cannot be derived from these amplitudes. Graphically (Fig. 1), the principal axes of the phase tensor ellipse are of lengths $\Phi_{\max}$ and $\Phi_{\min}$ and one of these axes is in the strike direction. The reference axis in this case is aligned with the direction of the major axis of the ellipse ($\beta_\Phi = 0$).

3-D structure

In the presence of a 3-D regional structure, all of the components and invariants of the phase tensor are, in general, non-zero. The graphical representation of the phase tensor (Fig. 1) differs from the 2-D case in that the principal axis of the ellipse is now at an azimuth given by $(\alpha_\Phi - \beta_\Phi)$ and is no longer aligned with the reference axis. The values of β_Φ may be regarded as a measure of departure from the condition for 2-D; the greater the value of β_Φ, the greater the deviation from the simple 2-D case. For small values of β_Φ, however, the error introduced by adopting conventional strike angles, derived assuming $\beta_\Phi = 0$, will be small, suggesting there will be 3-D conditions under which conventional 2-D approximations may not introduce significant error.

The phase tensor properties may also provide an indication of the presence of complicated conductivity variations in the earth. Taking the determinant of eqs (10) and (16)

$$\det(\mathbf{\Phi}) = \det(\mathbf{Y})/\det(\mathbf{X})$$

$$= \Phi_{\max}\Phi_{\min}. \tag{25}$$

A negative determinant of the phase tensor requires that either $\Phi_{\max}$ or $\Phi_{\min}$ be negative or, equivalently, one of the phase angles, $\tan^{-1}(\Phi_{\max})$ or $\tan^{-1}(\Phi_{\min})$, must lie outside the range 0–90 degrees. Conductivity distributions that give rise to this condition are extreme but by no means impossible (e.g. Egbert 1990). Such anomalous phases have been observed in the Andean subduction zone (Lazaeta & Haak 2003), for example, and Heise & Pous (2003) have modelled these extreme phases using an anisotropic layering in the presence of large resistivity variations. When anomalous phases are present, eq. (25) requires either $\det(\mathbf{X})$ or $\det(\mathbf{Y})$ to be negative, corresponding to $\tan^{-1}(\Phi_{\max}) > 90$ or $\tan^{-1}(\Phi_{\min}) < 0$, respectively. It is interesting to note that Lilley's (1998) defining criterion for 'a regular impedance tensor' requires these determinants to be positive.

Physically, the condition for $\det(\mathbf{X})$ or $\det(\mathbf{Y}) = 0$ corresponds to the in-phase (or quadrature) components of the electric field becoming independent of the direction of the magnetic field. In each case the phase ellipse collapses into a line. Anomalous phases ($\det(\mathbf{\Phi}) < 0$) occur when either the real or imaginary component of the electric field lies at an angle greater than 90 degrees from its expected direction in a uniform earth. The electric field thus

has a component in the opposite direction from that in a uniform half-space. The procedure for plotting the phase ellipse given in the Appendix can still be applied, but care is required in the interpretation, as one of the axes has negative values. Data for which the phase tensor has a negative determinant should be treated with caution.

To summarize: the dimensionality indicated by an impedance tensor (single site, single period) is given by invariants β_Φ and λ. Both β_Φ and λ are well defined provided $\det(\Phi)$ is finite and non-zero.

(i) The necessary conditions for 3-D is given by non-zero β_Φ (or $|\beta_\Phi| > \beta_c$, β_c selected as an appropriate threshold and/or error condition);

(ii) The necessary conditions for 2-D requires $|\beta_\Phi| < \beta_c$ and non-zero value of λ ($\lambda > \lambda_c$, λ_c selected as an appropriate threshold and/or error condition);

(iii) The necessary conditions for 1-D is both $|\beta_\Phi| < \beta_c$ and $\lambda < \lambda_c$.

If $\det(\Phi)$ is negative, one of the principal phase angles passes outside the range $0°$ to $90°$.

The criteria provided by the phase tensor are necessary (but not sufficient) conditions for determining the dimensionality of the regional conductivity structure. The phase tensor at a single period, under suitable conditions of symmetry, can have the characteristics of a lower dimension than that of the regional structure. Thus for example, the impedance tensor for a site that lies along an axis of symmetry of a 3-D structure can display 2-D characteristics, although neighbouring sites could appear 3-D. In essence, the dimensionality of the phase tensor must be evaluated taking into account the data at adjacent periods and neighbouring locations.

SOLUTIONS FOR THE REGIONAL IMPEDANCE TENSOR

Previous approaches to the problem of solving for the regional impedance tensor (G&B, Smith 1995) have mixed two quite distinct problems: one is soluble without any assumption, while the other requires constraints or assumptions to determine a solution. The phase tensor represents the soluble part of the problem. We describe below how the assumptions made to solve the combined problem affect both portions of the solution and impose unnecessary restrictions on the phase tensor.

The full set of (eight) equations for the (unknown) regional impedance and distortion tensors are represented by eq. (6). As the set of equations is underdetermined (eight equations in 12 unknowns), the first step taken by both G&B and Smith (1995) is to make the assumption that the regional structure is 2-D. This assumption sets four components of the regional impedance tensor to zero when the axes are rotated into the (unknown) strike direction, thereby reducing the number of unknowns by three. An undesirable consequence of this assumption is that one of the determinable parameters of the phase tensor (represented by β_Φ) is inadvertently set to zero. To obtain a solution it is still necessary to make two further assumptions concerning the form of the distortion tensor. G&B and Smith (1995) differ in their choices of these assumptions, but in both methods the number of unknown parameters is reduced to seven and the original underdetermined set of equations becomes an over-determined set.

Recognizing that the phase tensor is a partial solution of the full distortion problem allows a simpler approach. In particular, the as-

sumptions necessary to derive a solution can be made consistent with the information contained in the phase tensor.

Once the phase tensor is known, the equations for the regional impedance tensor (eq. 8) can be written as

$$\mathbf{X} = \mathbf{D}\,\mathbf{X_R}, \tag{26a}$$

$$\mathbf{Y_R} = \mathbf{X_R}\Phi. \tag{26b}$$

The non-unique nature of the problem is clearly apparent in eq. (26a), which is a set of four equations in eight unknowns. No solution is possible without constraints on either the form of the distortion tensor or the impedance tensor (or both). Once the distortion tensor is known, the regional impedance can be simply derived using

$$\mathbf{Z_R} = \mathbf{D}^{-1}\,\mathbf{Z} = \mathbf{D}^{-1}\mathbf{X}(\mathbf{I} + i\,\Phi). \tag{27}$$

The key to solving eq. (26) is to use the information provided by the phase tensor on the dimension of the regional structure (including, when appropriate, the strike direction). Thus it is possible to analyse the problem according to the previously determined dimensionality. The number of assumed parameters required is a function of this dimension.

1-D structure ($\beta_\Phi = 0$ and $\lambda = 0$)

Substituting the 1-D form of the regional impedance tensor (eq. 18) into eq. (26a) gives

$$\mathbf{X} = g\,\mathbf{D}\begin{bmatrix} 0 & 1 \\ -1 & 0 \end{bmatrix}, \tag{28}$$

where g is the unknown real part of the 1-D regional impedance tensor ($g = X_{1D}$). This is a set of four equations in five unknowns, which can be solved to within a single unknown multiplicative constant g. From eq. (28)

$$g\mathbf{D} = \mathbf{X}\begin{bmatrix} 0 & -1 \\ 1 & 0 \end{bmatrix}. \tag{29}$$

Note that the form of the distortion tensor is determined by eq. (29). When plotted as an ellipse, the orientation and aspect ratio of the distortion ellipse are known although the size of the ellipse is unknown. Equivalently, β_D, D_{min}/D_{max} (invariants) and α_D (not invariant) are known, although the magnitude of D_{min} or D_{max} is undetermined.

The scale constant g is essentially an unknown 'static shift' that can be applied to the apparent resistivity sounding curve after the removal of the determinable part of the distortion. This unknown constant can be determined by the use of external information, provided, for example, by a TEM sounding at the measurement site. However, without external information the scale is unknown and the magnitude can be set by applying a constraint on $\mathbf{D}$. To avoid dependence on the coordinate system in which the impedance tensor is represented, it is desirable for the chosen constraint to be placed on an invariant of $\mathbf{D}$. Furthermore, constraints should be chosen to be compatible with the case of no distortion. Possible choices include $\text{trace}(\mathbf{D}) = 2$, $\det(\mathbf{D}) = 1$ or $||\mathbf{D}||^2 = 2$ where $||\mathbf{D}||$ is the Frobenius norm. Each of these provides a scale to the distortion tensor. These give, respectively,

$$g = (X_{12} - X_{21})/2, \qquad g = \det(\mathbf{X})^{1/2} \quad \text{or} \quad g = ||\mathbf{X}||/\sqrt{2}. \tag{30}$$

It is also possible to derive a solution for $\mathbf{D}$ using the $\mathbf{Y}$ component of the impedance tensor using the same procedure. In practice, where β_Φ and λ contain noise (so that $|\beta_\Phi| < \beta_c$ and $\lambda < \lambda_c$) both

components can be used to derive estimates of the distortion tensor at any given period.

Choosing a constraint on the form of **D** is equivalent to assuming something of the nature of that distortion. The influence of variations in the near-surface electrical structure on the electric field vector has an analogue in the (tensor) multiple-source dipole–dipole resistivity method (e.g. Bibby *et al.* 1998). Modelling of tensor dc resistivity for shallow heterogeneities within an otherwise uniform resistivity background (Bibby & Hohmann 1993) shows that, close to the disturbing body, although the electric field is disturbed (distorted), the determinant of the apparent resistivity tensor is virtually unchanged from that of the surroundings. The equivalent in MT surveying would suggest that the determinant of the impedance tensor should remain nearly constant under distortion, provided the measurement site does not lie within the heterogeneity. The condition on the distortion tensor that achieves this is det(**D**) = 1. This forms one of our preferred conditions.

The solutions given by eq. (30) provide the basis of a simple but rigorous technique for distortion removal that can be applied to any sounding curve that contains a 1-D section. The distortion tensor can be determined for each period within the 1-D section and an appropriately weighted mean determined. The distortion can then be removed from the longer period part of the curve, irrespective of its dimension.

Anisotropic structures form a special case. In a horizontally anisotropic earth the phase tensor is indistinguishable from that of an isotropic half-space (CBB) although the apparent resistivity will differ along the axes of anisotropy. As a consequence the variation of apparent resistivity with azimuth is indistinguishable from the effects of local distortion. The identification of anisotropy would require measurements at several sites and would be indicated by the apparent distortion tensor being independent of location.

2-D structure ($\beta_\Phi = 0, \lambda \neq 0$)

Where the phase tensor analysis indicates that an MT sounding has no 1-D section, it may be necessary to seek a solution using a 2-D section of the sounding. The phase tensor not only provides confirmation of 2-D conditions it also provides an estimate of the principal axes of the regional impedance tensor, $\psi = \alpha_\Phi$. Rotating eq. (8) to the principal axes, the real part of the impedance tensor **X**' can be written

$$\mathbf{X}' = \mathbf{R}(\alpha_\Phi)\mathbf{X}\,\mathbf{R}^{\mathrm{T}}(\alpha_\Phi) = \mathbf{R}(\alpha_\Phi)\,\mathbf{D}\,\mathbf{X_R}\,\mathbf{R}^{\mathrm{T}}(\alpha_\Phi)$$
$$= \left[\mathbf{R}(\alpha_\Phi)\,\mathbf{D}\,\mathbf{R}^{\mathrm{T}}(\alpha_\Phi)\right]\mathbf{R}(\alpha_\Phi)\,\mathbf{X_R}\,\mathbf{R}^{\mathrm{T}}(\alpha_\Phi) = \mathbf{D}'\,\mathbf{X}'_{\mathbf{R}}$$
$$= \mathbf{D}'\begin{bmatrix} 0 & X_{//} \\ X_\perp & 0 \end{bmatrix}, \tag{31}$$

where $\mathbf{D}' = \mathbf{R}(\alpha_\Phi)\,\mathbf{D}\,\mathbf{R}^{\mathrm{T}}(\alpha_\Phi)$ is the distortion tensor relative to axes aligned in the direction of the strike, and $X_{//}$ and $X_\perp$ are the principal components of the regional impedance tensor parallel and perpendicular to the strike. This is a set of four equations in six unknowns (four components of **D**' and the two principal values $X_{//}$ and $X_\perp$). There is no unique solution. In order to solve eq. (31) two assumptions are required, one more than for the 1-D case. In essence, the necessary constraints can be regarded as unknown scale factors on each of the two principal components of the regional impedance tensor (Smith 1995). Note that, although for 1-D structure TEM soundings can provide the external information necessary to estimate the unknown scale factor, a TEM sounding is not sufficient when the near-surface structure is 2-D.

In practice when the data contain errors, the distortion tensor will be sought using a band of periods for which the phase tensor indicates 2-D conditions and the estimated strike is nearly constant. It is thus desirable that constraints on **D**' should not be dependent on the calculated strike direction (and consequently on the coordinate system). That is, it is desirable for conditions to be placed on the invariants of **D**'. By applying two constraints, eq. (31) is reduced to four unknowns and explicit expressions can be derived for these parameters. Any combination of invariants of **D** could be assigned values to derive a solution of eq. (31). This could include, for example, assigning det(**D**), trace(**D**) or β_D. Note that the condition $\beta_D = 0$ is equivalent to that used by Zhang *et al.* (1993), that the distortion tensor itself has a 2-D form. Setting the two constraints to be

$$\det(\mathbf{D}) = P \text{ and } \mathrm{trace}(\mathbf{D}) = T \tag{32}$$

gives

$$X_{//} = 2\,X'_{12}/[T - S] \text{ and } X_\perp = 2\,X'_{21}/[T + S], \tag{33}$$

where $S^2 = [T^2 + 4\,P X'_{12} X'_{21}/\det(\mathbf{X}')]$.

The distortion tensor, from eq. (31), is given by

$$\mathbf{D}' = \mathbf{X}'\begin{bmatrix} 0 & 1/X_\perp \\ 1/X_{//} & 0 \end{bmatrix}. \tag{34}$$

The requirement that S^2 is positive limits the choice of the values of P and T. In particular it is possible that setting $P = 1$ and $T = 2$ (consistent with no distortion) could be incompatible. In practice, as any choice of constraint on **D**' is equally valid, the value of one of the parameters will be set and the other chosen to satisfy the condition that $S^2 > 0$ for all the periods selected for the analysis. Note that there are two solutions given by eq. (33), which depend on the choice of the sign of S. Changing the sign of S effectively interchanges the scale factors in eq. (33).

Unlike the 1-D solution, the form of the distortion tensor can vary according to the constraints chosen. In particular, the directions of $D_{\max}$ and $D_{\min}$ will vary with the constraint used and consequently the derived distortion tensor does not necessarily provide any information relating to the conductivity gradients that give rise to that distortion.

The distortion analysis techniques of G&B and Smith (1995) also introduce constraints on **D**', although indirectly and each of a slightly different form. A major point of difference between these techniques and the phase tensor approach is that the dimensionality of the regional structure is not assessed prior to analysis but is assumed to be 2-D. The constraints used in these methods are only formally applicable when the 2-D assumption is valid (the case considered here).

G&B write **D**', the distortion tensor rotated to the strike direction, in the form of a product of 'twist' and 'shear' matrices. Such a description is coordinate dependent, and requires the coordinate axes to be specified for the description to be valid. The G&B form of distortion tensor is equivalent to setting two conditions on **D**':

$$\mathrm{trace}(\mathbf{D}') = 2 \text{ and } g_x = g_y, \tag{35}$$

where $g_x = (D'^2_{11} + D'^2_{21})^{1/2}$ and $g_y = (D'^2_{12} + D'^2_{22})^{1/2}$.

The second condition is not invariant and g_x, g_y will change when **D**' is expressed in any other coordinate axes. For 2-D situations, the G&B 'estimate' has an explicit form obtained by solving eq. (31) with the constraints of eq. (35).

$$X_{//} = 0.5[X'_{12} + X'_{21}R], \quad X_\perp = 0.5[X'_{21} + X'_{12}/R], \tag{36}$$

where $R = \mathrm{sign}(X'_{12} X'_{21})\,[(X'^2_{12} + X'^2_{22})/(X'^2_{11} + X'^2_{21})]^{1/2}$. The

sign is chosen in order to give the appropriate solution when no distortion is present. The explicit form of the distortion tensor can then be calculated from eq. (34).

Smith (1995) uses a similar approach to G&B except that the constraints are given by

$$g_x = g_y = 1. \tag{37a}$$

For comparison with G&B these constraints can be rewritten in the form

$$||\mathbf{D}||^2 = 2 \text{ and } g_x = g_y, \tag{37b}$$

where $||\mathbf{D}||$ denotes the Frobenius norm (an invariant). Like G&B only one of the conditions is invariant. For 2-D conditions, the explicit solution for the principal components of $\mathbf{X_R}$ using these constraints is

$$X_{//} = \left[X_{12}'^2 + X_{22}'^2\right]^{1/2}, \ X_\perp = \left[X_{11}'^2 + X_{21}'^2\right]^{1/2}. \tag{38}$$

It is important to stress that there is an infinite set of valid solutions all of which satisfy eq. (31) but which differ according to the constraints chosen. The inherent non-uniqueness of distortion removal in a 2-D situation can be demonstrated using synthetic data. For this purpose we use the 2-D example from McNeice & Jones (2001), which was also used by CBB to illustrate the properties of the phase tensor. Fig. 2(a) shows the real and imaginary parts of a synthetic 2-D regional impedance tensor $(\mathbf{X_R}, \mathbf{Y_R})$ using the ellipse representation (see Appendix). Note that the principal axes of the

$\mathbf{X_R}$ and $\mathbf{Y_R}$ ellipses are coincident and lie parallel and perpendicular to the strike of the regional structure (a necessary condition for 2-D structures). A distortion tensor (Fig. 2b) is applied resulting in the distorted (measured) impedance tensor shown in Fig. 2(c). The major axes of the two ellipses, representing the real and imaginary parts of the measured impedance tensor, are no longer parallel and neither is parallel to the strike direction. The aim of distortion analysis is to recover the regional impedance of Fig. 2(a) from the measured data of Fig. 2(c). The initial step in the analysis of the distorted data is to determine the phase tensor (eq. 10), which is shown in Fig. 2(d). As would be expected for noise free data in a 2-D situation, the value of β_Φ for the phase tensor is zero and the principal axes of the phase tensor are the same as those of the regional data (Figs 2a and d). Thus the regional strike direction is recovered exactly.

The non-unique step is the estimation of the distortion and regional impedance tensors. Fig. 3(a) shows a selection of estimates of the distortion tensor calculated using different constraints (see caption for details). For comparison, the original distortion tensor is also shown together with the G&B and Smith (1995) estimates. Note that for noise-free 2-D data, the latter two estimates differ from each other only by a scale factor. Figs 3(b) and (c) show the corresponding recovered impedance tensor components $(\mathbf{X_R}, \mathbf{Y_R})$. All choices of the constraints applied to the distortion tensor solution are equally valid. Although some of the resulting estimates of the regional impedance tensor approximate the original input data more

(a) Undistorted impedance tensor ellipses (b) Distortion tensor (c) Distorted impedance tensor ellipses (d) Phase tensor
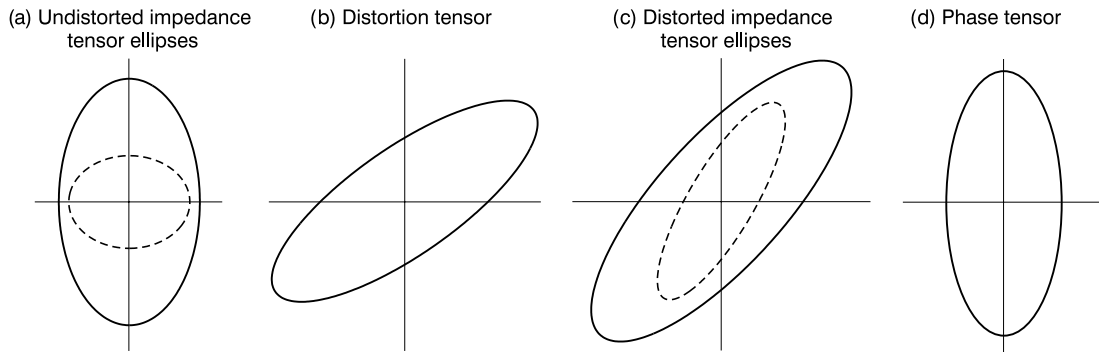
Figure 2. Demonstration of the effects of distortion using a synthetic example from McNeice & Jones (2001). (a) The regional impedance tensor plotted using the graphical representation (Fig. 1). The solid and dashed ellipses show the real and imaginary parts of the impedance tensor, respectively. (b) The distortion tensor ellipse. (c) The distorted impedance tensor ellipses (i.e. product of tensors of a and b). (d) The phase tensor derived from the distorted impedance tensor. Note that the principal axes of the phase tensor coincide with the principal axes of the regional impedance tensor.

(a) Distortion tensor estimates (b) Estimated impedance tensor ellipses (**X**) (c) Estimated impedance tensor ellipses (**Y**)
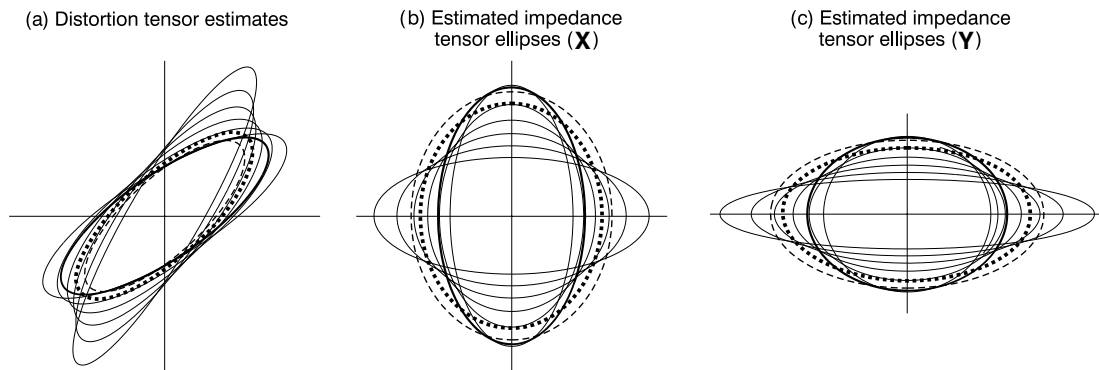
Figure 3. The non-uniqueness of the determination of the undistorted impedance tensor is demonstrated for the example shown in Fig. 2(a) Elliptical representation of a set of possible solutions for the distortion tensor (thin lines) derived using the coordinate invariant constraints det(**D**) = 1 and β_D with values varying between $\pm 12°$ (4° intervals). The bold ellipse is the applied distortion tensor (Fig. 2b) and the dotted and dashed ellipses are the estimates of the distortion tensor obtained using the constraints of G&B and Smith (1995), respectively. (b) and (c) show the corresponding solutions for the real (**X**) and imaginary (**Y**) parts of the impedance tensor.

closely than others, these estimates will correspond with a set of constraints that happen to match the form of the original distortion tensor. More importantly, however, there is no way of knowing *a priori* the form of the original distortion tensor. A set of constraints that recover the input data for this example will not necessarily provide the best estimate in any other situation.

3-D structure ($\beta_\Phi \neq 0$)

In a 3-D situation, there is no simplification to the form of the regional impedance tensor that can be applied to eq. (26). Four constraints are required to determine the regional impedance tensor and effectively no information can be obtained about the distortion tensor. Even when 3-D structures are present, the phase tensor ellipse in most instances has well defined principal axes (at an azimuth given by $\alpha_\Phi - \beta_\Phi$), which CBB suggest can be considered to be a generalization of the concept of strike direction to 3-D. The principal axes indicate the directions of greatest and least induction current at a given period, which, in 2-D, are parallel or orthogonal to the strike direction. In 3-D this may be considered to be the nearest one can come to determining a 'best' approximation to the 2-D strike. The greater the value of β_Φ, the greater is the deviation from simple 2-D symmetry. It is thus possible, when β_Φ is small, to proceed as though a principal axis of the phase tensor ellipse is the strike direction (the pseudostrike) and to make the same assumptions as were made to estimate the regional impedance tensor in 2-D, that is, assume that the real part of the regional tensor, $\mathbf{X_R}$, is antidiagonal in a coordinate system aligned with the principal axes of the phase tensor ellipse. One advantage of this procedure is that no distinction is needed between the approaches used in 2-D and 3-D situations. These assumptions provide two of the four necessary constraints required to obtain a solution to eq. (26). Note that, although $\mathbf{X_R}$ is assumed to have a 2-D form, the imaginary part $\mathbf{Y_R} = \mathbf{X_R}\Phi$ will not have an antidiagonal form (unless Φ indicates 2-D conditions). To complete the solution it is necessary to make assumptions on the form of the distortion tensor, as was required for 2-D analysis. Although a solution for $\mathbf{X_R}$ may be obtained, the appropriateness of 3-D distortion analysis is questionable.

DIMENSIONALITY AND DISTORTION REMOVAL—FIELD EXAMPLES

To demonstrate the use of the phase tensor for dimensional analysis and the consequential removal of distortion we use data from a site on the eastern side of the Taupo Volcanic Zone of New Zealand. Fig. 4 shows plots of the apparent resistivity and phase from a site where the apparent resistivity curves are not coincident at small periods. The corresponding phase tensor is shown in two forms. Fig. 5 shows elliptical representations of the phase tensor for every second period of the curve of Fig. 4. An alternative representation of the phase tensor is given in Fig. 6, which shows the invariant parameters of the phase tensor that reflect the dimensionality of the regional (or undistorted) structure. Fig. 6(a) (upper plot) shows the ratio $\lambda = (\Phi_{max} - \Phi_{min})/(\Phi_{max} + \Phi_{min})$, which will be zero in 1-D conditions, and Fig. 6(b) (central plot) shows values of β_Φ (in degrees), the measure of 2-D/3-D structure. Fig. 6(c) (lower curve) shows the azimuth of the maximum of the phase tensor plotted for periods when the structure is not 1-D. The direction of this axis corresponds to the direction of the major axes of the ellipses shown in Fig. 5.

Although the values of λ are small at the shortest periods, they do not lie within one standard error of zero. This characteristic of small, but not exactly zero, λ at the early part of the curves is typical of almost all the measured data from the Taupo area. The small difference from zero is surprising and suggests either that the assumption of purely galvanic distortion is incorrect, or possibly, that some small systematic error (or bias) is present in the measurement, so that the error bounds may be under estimated. For the purposes of distortion analysis we have categorized values of $\lambda < 0.1$ as 1-D. The next section of the curve, extending to periods of about 10 s, shows 2-D characteristics, with small values of β_Φ, ($<1.5°$) and $\lambda > 0.1$. At periods >10 s, β_Φ becomes $>1.5°$, although the principal axis of the phase tensor ellipse occurs at a near constant azimuth.

1-D analysis. 1-D distortion analysis has been applied to data from the first six periods. As 1-D conditions are not met exactly, separate estimates were made using both the $\mathbf{X}$ and $\mathbf{Y}$ components at each period, using the condition that $\det(\mathbf{D}) = 1$. The derived distortion tensors (from both $\mathbf{X}$ and $\mathbf{Y}$) are shown in a single plot in Fig. 7. An indication of the validity of the approach is the consistency of the individual estimates at each period and between the estimates based on $\mathbf{X}$ and $\mathbf{Y}$ components. This consistency starts to breakdown if more periods are included when the 1-D approximation becomes invalid. The distortion tensor (in the measurement coordinate system) derived from the mean of individual estimates for $T < 0.02$ s, after weighting each estimate by its computed variance, is given by

$$\mathbf{D} = \begin{bmatrix} 1.07 & -0.04 \\ -0.02 & 0.93 \end{bmatrix} \pm \begin{bmatrix} 0.02 & 0.01 \\ 0.02 & 0.02 \end{bmatrix}. \tag{39}$$

The small off-diagonal terms suggest that the distortion is almost purely an amplitude change to the components expressed in the measurement coordinates. The regional impedance tensor is derived from eq. (28) with the appropriate scale factor g (from eq. 30) and the resulting sounding curves are shown in Fig. 8. The estimated errors in the apparent resistivities are slightly larger than in the measured data (Fig. 4a) reflecting the uncertainty in the distortion tensor. The presence of asymmetry in the distortion tensor will result in a change in the shape of the sounding curve in all coordinate systems, which cannot be reproduced static shifts alone. The phases (Fig. 8b) are almost unchanged in the process. The difference between ρ_{xy} and ρ_{yx} apparent resistivities at small periods is eliminated by the distortion removal, although there is still an unknown scale factor or site gain that can be applied to the impedance tensor at all periods. The site gain can only be determined from independent data, such a TEM soundings or using data from surrounding sites (e.g. Ogawa & Uchida 1996).

2-D analysis: If a sounding contains a 1-D section then distortion analysis would normally be applied to that portion of the sounding. However, there will be soundings that contain no 1-D section and distortion analysis of a 2-D section of the curve will be necessary. To illustrate 2-D analysis we use a 2-D section of the sounding of Fig 4. Analysis was applied to the section $0.12 < T < 1.2$ s, which shows 2-D character ($\beta_\Phi < 1.5°$) and near constant azimuth of the phase tensor maximum (strike direction $\approx -78°$). The invariant constraints $\det(\mathbf{D}) = 1$ and trace $(\mathbf{D}) = 2.1$ were used, where the value of the trace was selected to ensure that S^2 of eq. (33) is positive at all the periods of the selected range. The resulting estimates of the distortion tensor, shown in Fig. 9, are almost constant with period. The mean value of the distortion tensor derived with these constraints gives

$$\mathbf{D} = \begin{bmatrix} 0.83 & -0.25 \\ -0.21 & 1.27 \end{bmatrix} \pm \begin{bmatrix} 0.01 & 0.01 \\ 0.01 & 0.01 \end{bmatrix}. \tag{40}$$

APPARENT RESISTIVITY
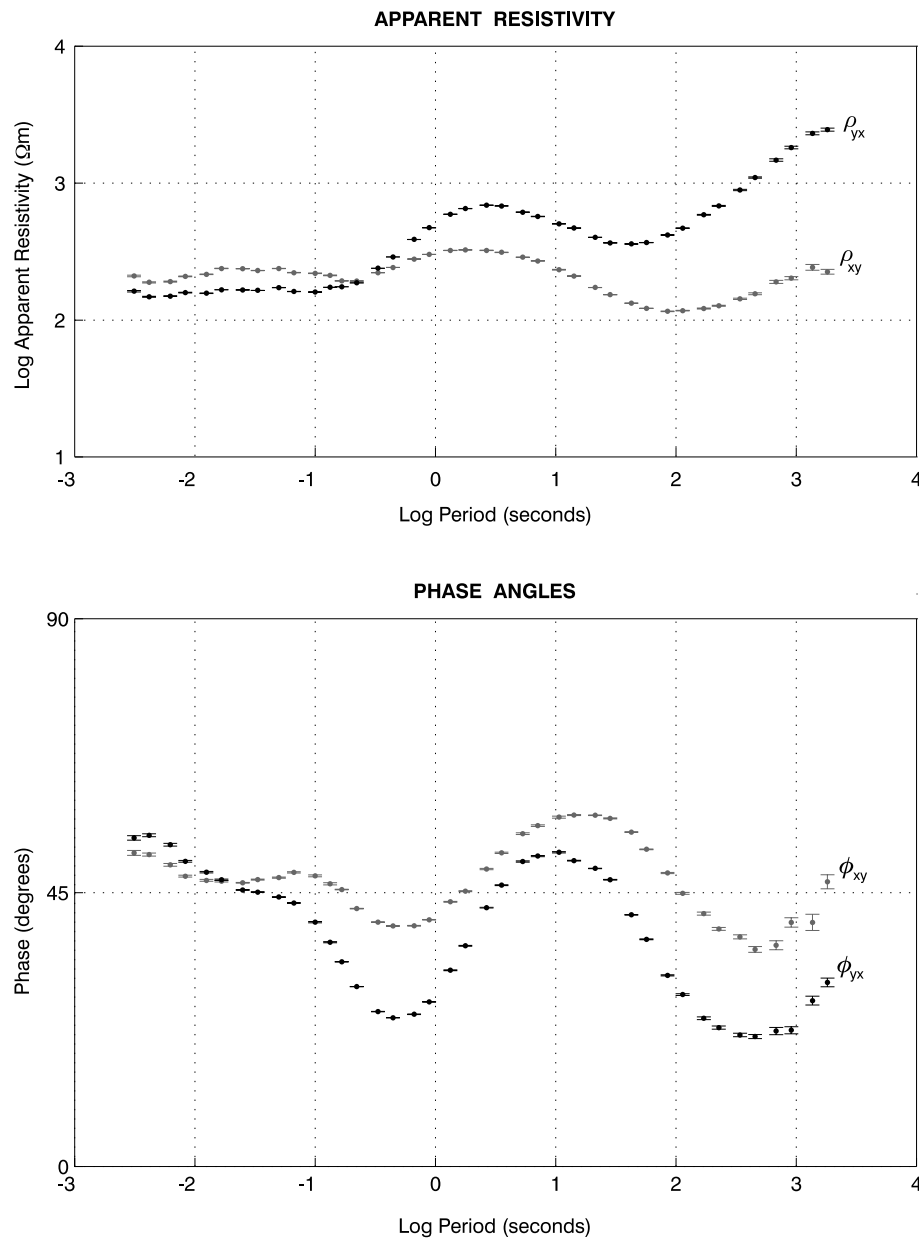
Figure 4. Magnetotelluric sounding curve for a site near the Taupo Volcanic Zone, showing the *xy* and *yx* apparent resistivity and phases in the measurement coordinate system (aligned magnetic north and east).
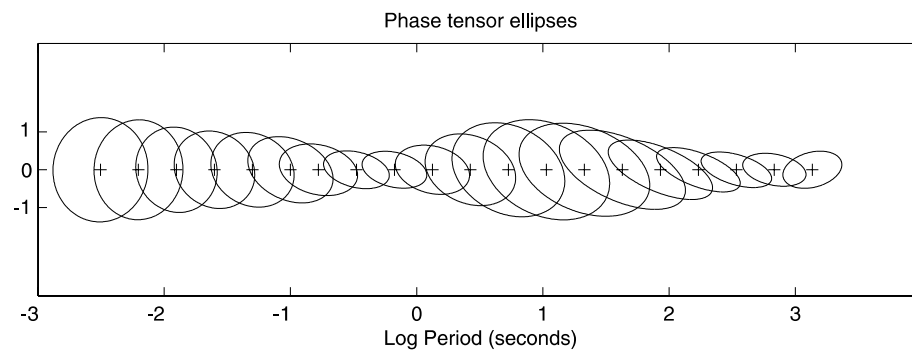
Figure 5. Phase tensor ellipses plotted for every second data point of the MT sounding shown in Fig. 4. A radius of unity corresponds to a phase of 45 degrees. Near-circular phase tensor ellipses at short periods are indicative of near 1-D structure. At longer periods the figures are more elliptical with clearly defined principal axes.
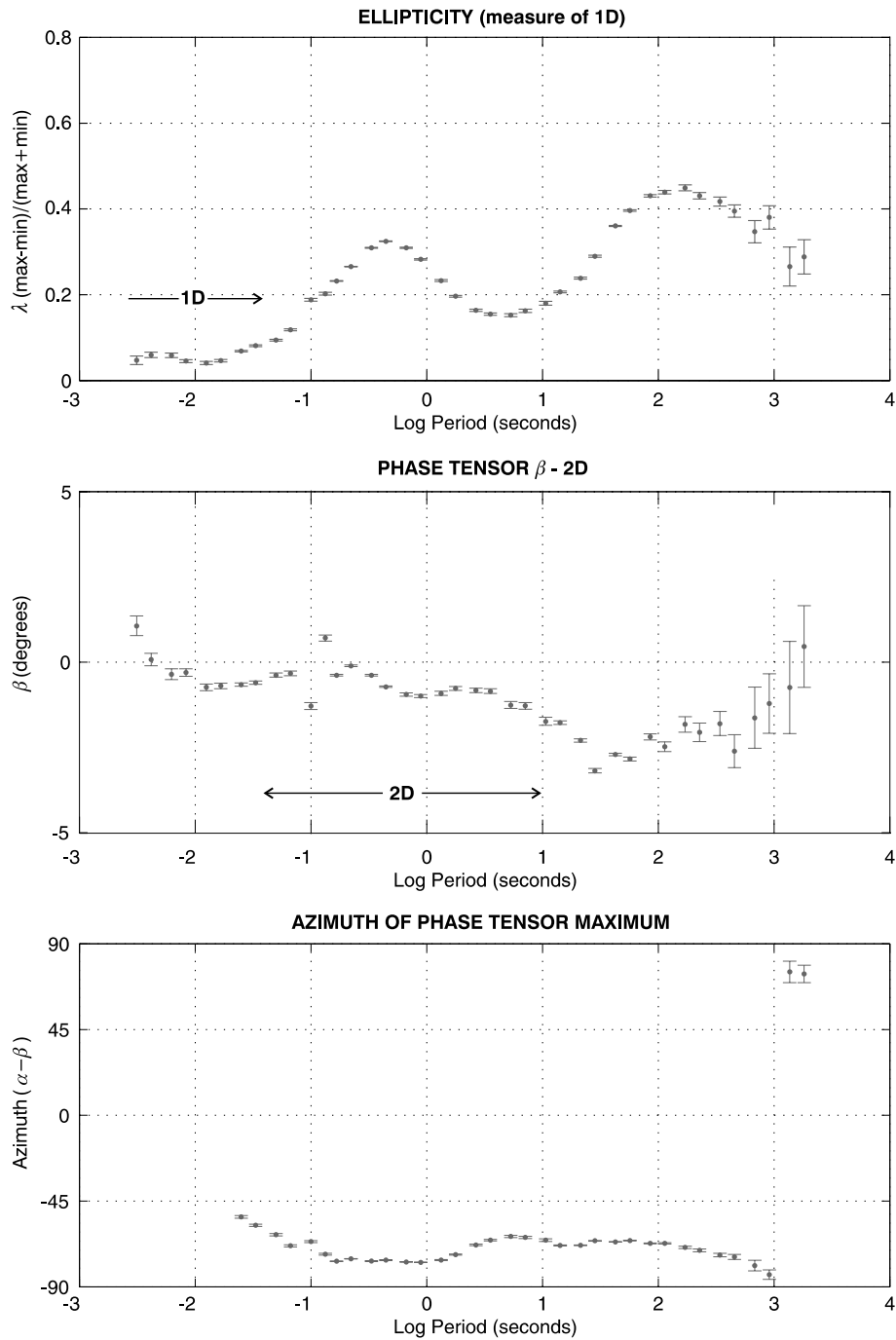
Figure 6. Parameters of the phase tensor for the data of Fig. 4. (a) The (coordinate invariant) phase tensor ellipticity $\lambda = (\Phi_{max} - \Phi_{min})/(\Phi_{max} + \Phi_{min})$. 1-D structure is indicated by (near) zero values of λ. (b) The phase tensor skew angle β_Φ, which is zero for 2-D structure. (c) The azimuth of the major axis (Φ_{max}) of the phase tensor ellipse, plotted for data where $\lambda > 0.1$.

The distortion tensor derived from the 2-D analysis would not be expected to match that derived from the 1-D analysis, as an additional constraint has been applied. When the distortion is removed (Fig. 10) the two curves do not coincide within the section used to determine the distortion tensor. Indeed the separation of the curves will be a function of the constraints used. In this example it is possible to compare the 2-D distortion removal with the 1-D case. For a sounding with no 1-D section this would not be possible. In general, the curves will not coincide within a 2-D section and there is no means of gauging the relative scale for the apparent resistivity. In coordinates aligned with the principal axes of the 2-D section, the shapes of the curves are uniquely determined but each curve can be offset parallel to itself by an indeterminate amount. In this example the added information from the 1-D section is sufficient to fix the curves relative to one another, although the absolute value cannot be determined from the MT sounding alone. This use of 2-D analysis followed by adjustment of the curves using a 1-D portion of the MT curve was proposed by Groom & Bahr (1992). However, if a 1-D section is present, 1-D analysis is the most effective approach.

1D distortion tensor ellipses
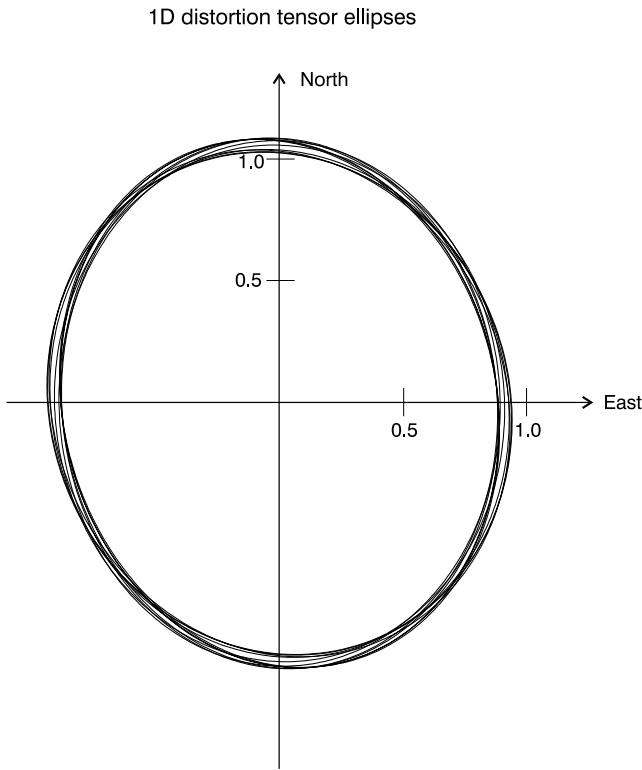
Figure 7. Superimposed plots of the distortion tensor ellipses derived from the approximately 1-D section of the MT sounding (first six periods, Fig. 4) showing the consistency between the estimates at each period. The distortion tensors are determined using the constraint det(**D**) = 1.

INSTALLATION ERROR AND APPARENT DISTORTION

Errors during installation or inaccurate alignment of sensors in the field can appear as an apparent distortion when the resulting data are analysed. The influence of these errors can be simply calculated. Assuming the azimuth of the electric field measurement dipoles are misaligned by angles ε_x and ε_y then the measured electric field vector $\mathbf{E}'$ is related to the true electric field $\mathbf{E}$ by the relationship

$$\mathbf{E}' = \begin{bmatrix} \Delta_x \cos \varepsilon_x & \Delta_x \sin \varepsilon_x \\ -\Delta_y \sin \varepsilon_y & \Delta_y \cos \varepsilon_y \end{bmatrix} \mathbf{E}$$
$$= \mathbf{D}\,\mathbf{E}, \tag{41}$$

where Δ_x and Δ_y are the ratios of the lengths of the assumed electrode spacing to the actual line length. This equation is identical in form to the galvanic distortion given in eq. (1). The effect of inaccurate electric field sensor installation is indistinguishable from the distortion produced by near-surface galvanic effects and can be dealt with, and corrected for (removed) in a similar way. Care is required in the choice of constraints as apparent distortion caused by installation errors can have characteristics that could be incompatible with some forms of constraint. For example, the reversal of one electric field line ($\varepsilon_x = \pi, \varepsilon_y = 0$) gives an apparent distortion tensor with a negative determinant. Thus, the constraint det(**D**) = 1 would be inappropriate. When dealing with installation error the most robust form of constraint is the Frobenius norm $||\mathbf{D}||^2 = 2$. Note that the condition for **D** to be singular, when the distortion problem has no solution, is given by $\cos(\varepsilon_x - \varepsilon_y) = 0$, which corresponds to the electric field lines being parallel, a situation that may accidentally occur with certain electrode configurations.

Misalignment of the magnetic sensors will produce a signature, which cannot be removed quite so simply. Assuming magnetic coils are misaligned by angles ζ_x and ζ_y, the measured magnetic field, $\mathbf{H}'$, is given by

$$\mathbf{H}' = \begin{bmatrix} \cos \varsigma_x & \sin \varsigma_x \\ -\sin \varsigma_y & \cos \varsigma_y \end{bmatrix} \mathbf{H}$$
$$= \mathbf{C}\,\mathbf{H}, \tag{42}$$

where **H** is the magnetic field that would be recorded if the sensors were correctly aligned. In this case the phase tensor **Φ** does not eliminate the error. The corresponding modified phase tensor **Φ**′ is given by

$$\mathbf{\Phi}' = \mathbf{C}\,\mathbf{\Phi}\,\mathbf{C}^{-1}. \tag{43}$$

In a 1-D situation the phase tensor is unchanged by magnetic sensor misalignment, but in 2-D the influence on the phase tensor is such that the apparent dimensionality of the structure can be changed. In particular, β_Φ, which would be expected to be zero for 2-D regional structure will not be zero. Furthermore, since β_Φ is a function of the components of **Φ**′ its value will vary with period so that the effect of misalignment on the phase tensor is could be mistaken for the effects of a 3-D regional structure. Modern MT instrumentation and data processing are rapidly approaching the point where the alignment of receivers can be a significant contribution to the total measurement error.

Field example

Fig. 11 shows the component apparent resistivity sounding curves from sites 600 m apart (sites 100 and 110), adjacent to the Taupo Volcanic Zone (Ogawa *et al.* 1999). The sites are in a similar geological domain as that of the curve of Fig. 4. The second site (110, Fig. 11b) was occupied to overcome the poor data quality between 1 and 10 s (gap in Fig. 11a) caused by tree movement at the original location (100). However, data from the replacement site (Fig. 11b) had significant differences from that of the original site. Analysis suggests that phase tensor data for the two sites (Fig. 12) are the same within the (large) errors. For periods less than 0.1 s the data at both sites suggest (near) 1-D characteristics ($\lambda < 0.1$) allowing the use of 1-D distortion removal. For site 100 (Fig. 11a) the distortion tensor determined from the 10 shortest periods is within one standard deviation of the identity matrix, indicating no near-surface distortion is present at this site. There are less data within the 1-D section at site 110 (Fig. 11b) and the 1-D analysis can be applied at only the first six periods. The resulting distortion estimates (setting trace (**D**) = 2) are constant within errors at each period and give a mean distortion tensor of

$$\mathbf{D} = \begin{bmatrix} 1.13 & -1.12 \\ 0.85 & 0.87 \end{bmatrix} \pm \begin{bmatrix} 0.03 & 0.06 \\ 0.03 & 0.03 \end{bmatrix}. \tag{44}$$

The large values of the off-diagonal terms are indicative of a large rotational component to the distortion and suggest the 'distortion' may result from a blunder in the electric field installation rather than from the near-surface conductivity structure. From eq. (41), the apparent angular errors, ε_x and ε_y, can be derived from the ratios D_{12}/D_{11} and $-D_{21}/D_{22}$, which give angles of $-44.7°$ and $-44.3°$, respectively (twice the magnitude of the local magnetic declination) suggesting an installation blunder as the origin of the problem. The sounding curve (Fig. 11c) derived by applying the distortion removal matches that at the adjacent site within the standard errors, after allowance for the undetermined multiplicative constant. This

APPARENT RESISTIVITY WITH DISTORTION REMOVED

PHASE ANGLES
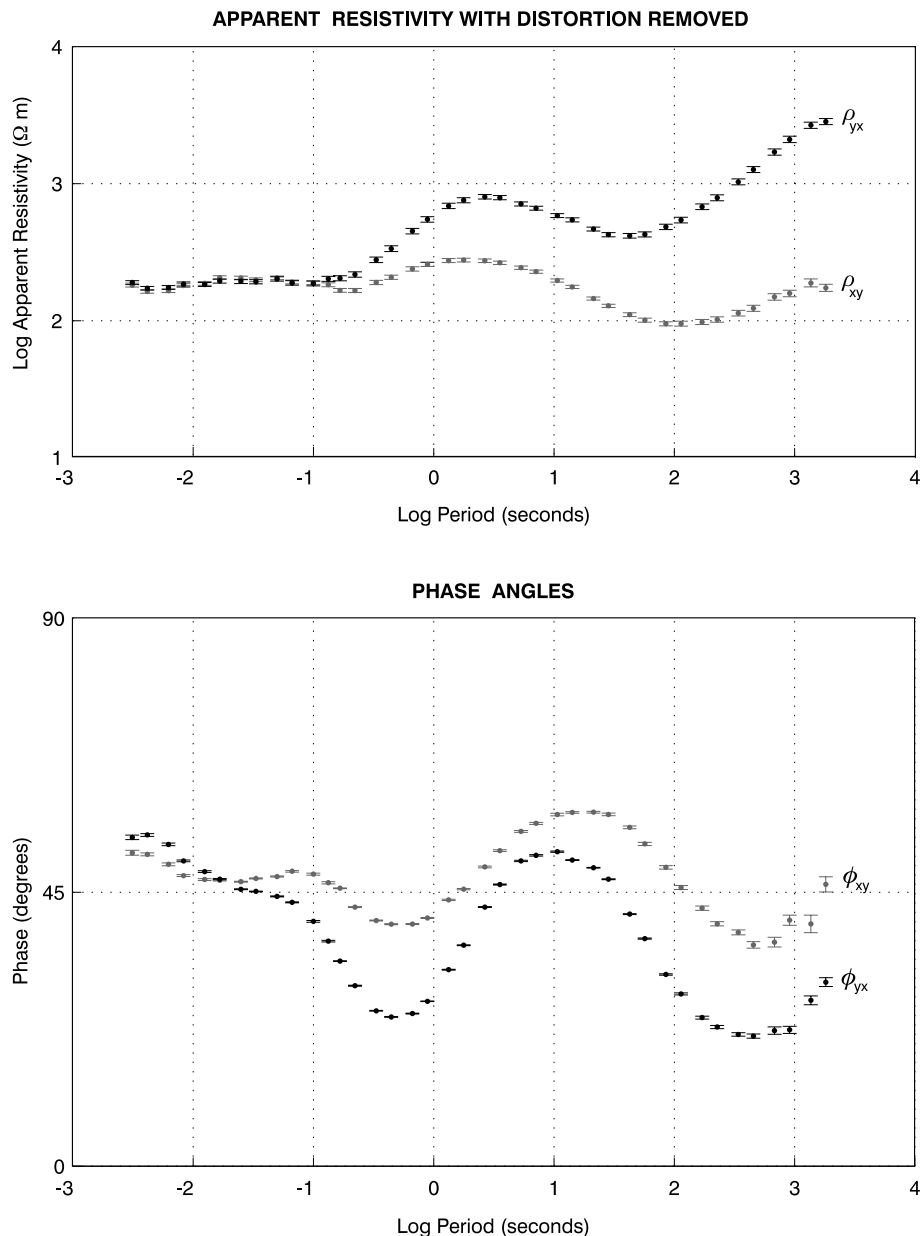
Figure 8. MT sounding of Fig. 4 after the removal of the distortion tensor derived from the 1-D section of the sounding. The distortion tensor used is the weighted mean of the individual estimates shown in Fig. 7. The value of the apparent resistivity is determined to within a single multiplicative constant.

example illustrates an extreme case of apparent distortion. We suggest that minor installation errors are a frequent cause of low level distortion.

DISCUSSION

The usual scenario envisaged in distortion analysis is the presence of small, near-surface, 3-D heterogeneities within an otherwise simpler (1 or 2-D) regional structure. At periods greater than some threshold the inductive currents caused by the heterogeneity become negligible and the response of the heterogeneities becomes frequency independent or galvanic. Once the near-surface response becomes galvanic, the phase tensor reflects the inductive response of the regional structure alone. Large-scale features can also be treated as distorters, and their influence removed from the longer period

portion of an MT sounding provided the inductive currents associated with these conductivity structures are negligible. Thus a MT sounding curve may be thought of as passing through a sequence of galvanic distorters each with a different characteristic length scale and different threshold period. Whether the response at a particular period range is treated as distortion or as a recoverable part of the resistivity structure may depend on the scale of the survey and the distribution of measurement sites. At the extreme, the upper crust may be considered as a galvanic distorter to the inductive response of the lower crust and mantle (e.g. Simpson 2001; Bahr & Simpson 2002).

The simple approach to MT soundings that appear to be 1-D at short periods and which are characterized by a portion of the apparent resistivity sounding curves, which are (near) parallel but not coincident, is to apply a 'static shift'. This involves displacing one or both curves so that the apparent resistivities are equal within the

2D distortion tensor ellipses
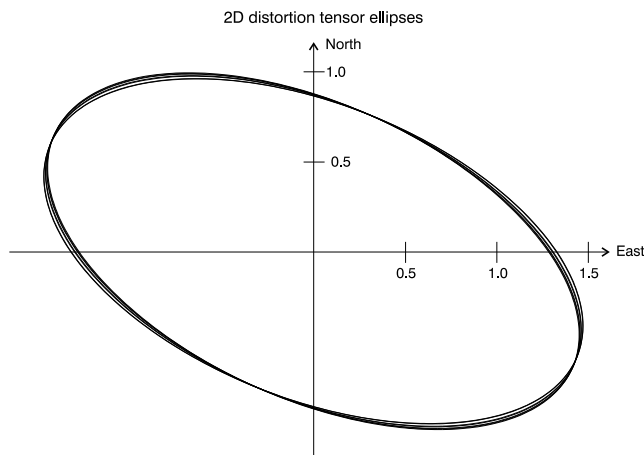
Figure 9. Distortion tensor ellipses derived from the approximately 2-D section of the MT sounding (Fig. 6), where the azimuth of $\Phi_{\max}$ (strike direction) is near constant at $\approx -78°$. (See text for details of the constraints used.) The ellipses are superimposed to show the variability between the estimates at each period. Because of the additional constraints required, the distortion tensors do not match those derived from the 1-D analysis (Fig. 7).

APPARENT RESISTIVITY WITH DISTORION REMOVED
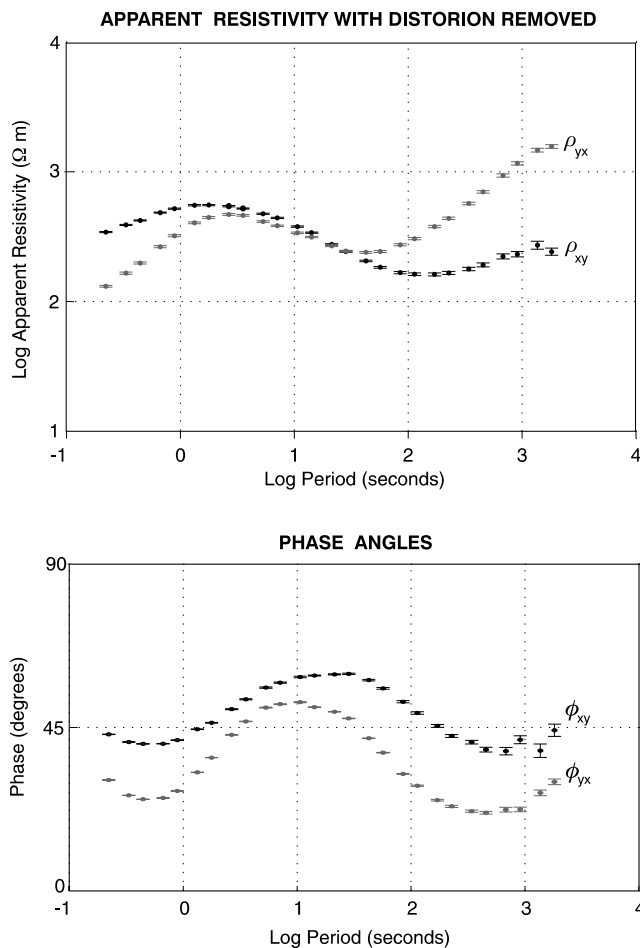
Figure 10. MT sounding curves of Fig. 4 after the removal of the distortion tensor derived from the weighted mean of the individual (2-D) estimates shown in Fig. 9. Note that the curves separate at small periods. This separation is a function of the constraints used in the analysis. The relative position of the curves is not fixed by 2-D analysis, nor is the absolute values of either of the principal components.

(assumed) 1-D section of the sounding. This is equivalent to applying an inverse distortion matrix which is diagonal in the coordinate system used (or symmetric in any other coordinate system). In general, however, the distortion tensor is not symmetric and the presence of distortion will change the shape of the both the phase and the sounding curves in any coordinate system. That is, part of the distortion cannot be removed by a static shift and this process alone will not correctly recover the shape of the curves. When TEM data is used to determine a scale correction for the apparent resistivity, the scaling should be applied after the distortion has been removed.

The methods of G&B and Smith (1995) have become standard methods for (simultaneously) determining both the 'strike' direction and for removing distortion. These techniques make assumptions that are strictly only applicable for 2-D resistivity structures, and tacitly treat as noise the determinable parameter that is indicative of 3-D conditions. There are disadvantages in combining the analysis of strike (uniquely determinable) and distortion (requiring constraints) for either single soundings or an array of sites (McNeice & Jones 2001). The greatest amount of information about the distortion tensor is found in a 1-D section of a sounding whereas the strike is only determinable from a 2-D section. As we have shown, the strike can be determined from the phase response alone and requires no knowledge of the distortion tensor. When the problems are combined, determinable parameters are lost as the solution for the distortion tensor is incomplete. Furthermore, the misfit resulting from over-constraining the solution in the 1-D section is treated as noise by this process. More information can be determined from the combination of the phase tensor analysis followed by formal distortion removal.

CONCLUSION

The distortion of the electric field caused by localized variations of conductivity is a ubiquitous problem in MT. Removal of the effects of galvanic distortion, where the cause of the distortion is unknown, is an underdetermined problem and cannot be solved uniquely. There is, however, a well-defined partial solution, the phase tensor, which represents four of the eight parameters needed to define the regional (undistorted) impedance tensor (CBB). The phase tensor is independent of the distortion and is simply expressed in terms of the observed impedance tensor components. Furthermore, it provides a simple and objective measure of the dimensionality of the MT response at any period. The remaining parameters required to fully define the regional impedance tensor (and the distortion tensor) cannot be uniquely determined without introducing assumptions or constraints. The number of determinable parameters of the regional impedance tensor and the number of constraints necessary to determine a solution depend on the minimum dimension of the regional conductivity structure.

In order to obtain the maximum amount of information on the regional (undistorted) impedance tensor we propose an approach that uses the information on the dimensionality provided by the phase tensor. We then apply the minimum number of constraints to the distortion tensor appropriate to near-surface dimensionality (or the minimum dimension). The greatest amount of information can be determined from a sounding, which contains a 1-D section from which the form (although not the magnitude) of the distortion tensor can be recovered. This allows the undistorted impedance tensor to be recovered to within a single multiplicative constant. It is only in the 1-D case that any information about the distorting field is recovered. In this case, the form of the distortion tensor, and in
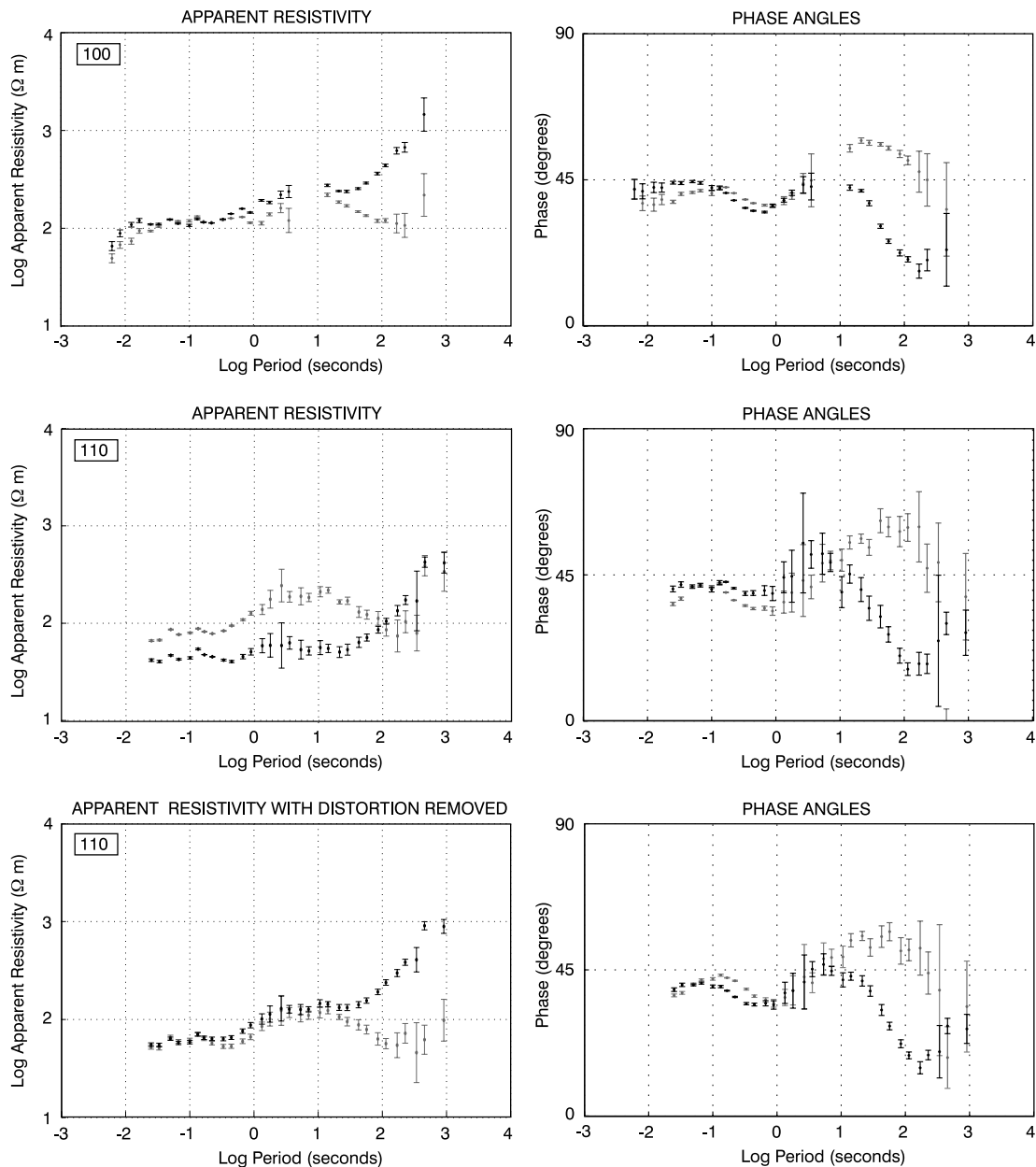
Figure 11. (a) and (b). Data from two MT soundings near the Taupo Volcanic Zone, 600 m apart. Site 110 (b) was omitted from analysis because of large apparent distortion. Data are shown for coordinate axes rotated to be parallel and perpendicular to the trend of the Taupo Volcanic Zone (azimuth of 45°). (c) Sounding curve (site 110) after distortion removal using the 1-D section of the curve. The revised data lie within a multiplicative constant (which is unconstrained in the distortion analysis) of the regional curve at the neighbouring site (a).

particular the orientation of the tensor maximum, will reflect the cause of the distortion.

When a sounding does not contain any coherent section that can be identified as 1-D, analysis can be applied to a section of higher dimension. However, when this occurs, the form of the derived distortion tensor is a function of the assumptions made to obtain a solution and thus it can provide no information on the cause of that distortion. Where a 2-D section of the sounding is used for the analysis, the impedance tensor can be determined to within two multiplicative constants, which represent unknown scale factors on each of the principal apparent resistivities. Where a sounding displays 3-D character throughout, there is no simplifying form of the

regional impedance tensor and the phase tensor is the only distortion free portion of the impedance tensor that can be recovered.

The problem of distortion removal is commonly misunderstood. It has become common practice to combine the problem of determining the strike direction with distortion removal. The phase tensor separates the problems, providing the maximum information on the implicit dimensionality of the impedance tensor and, when appropriate, an explicit solution for the strike direction. The use of the information provided by the phase tensor leads to a simple yet rigorous approach to the problem of distortion removal involving a minimum set of explicit assumptions. Distortion removal should be used as a routine process in the analysis of MT data.
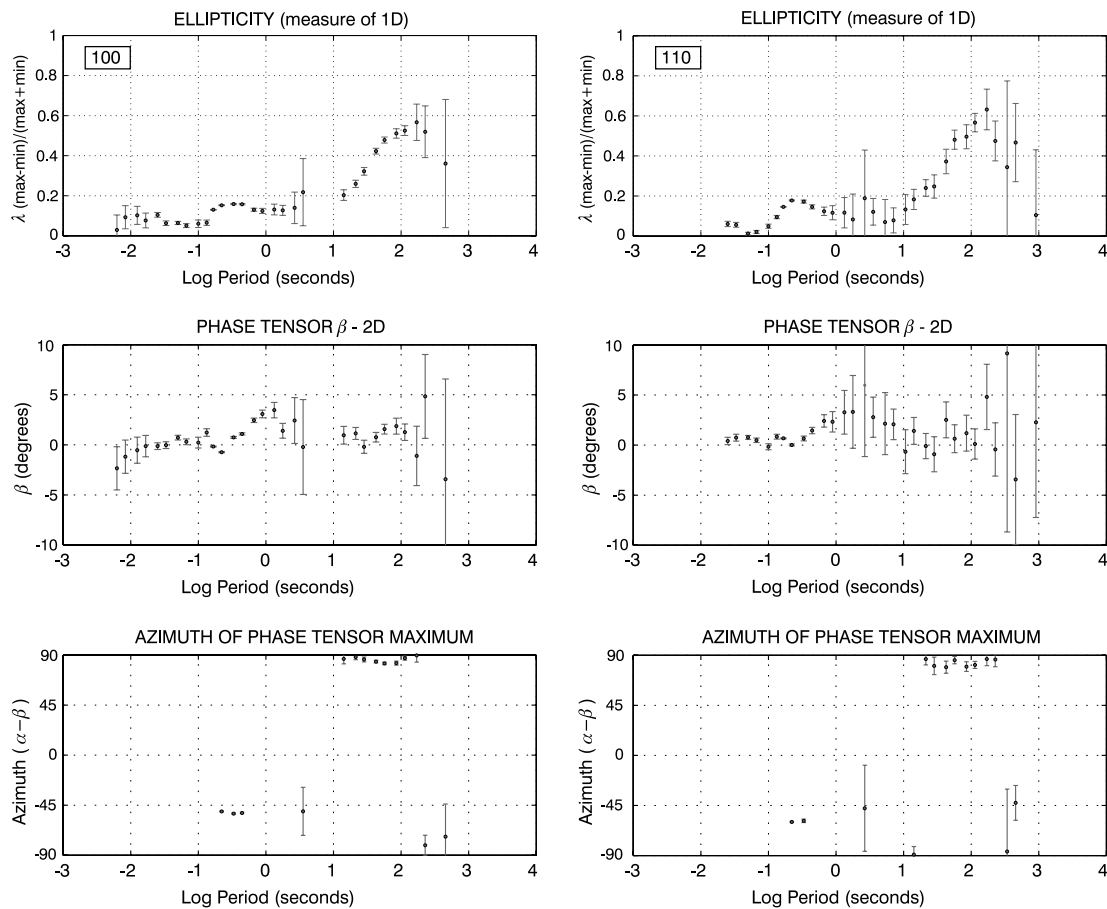
Figure 12. Phase tensor parameters for MT data from sites 100 and 110 (Fig. 11). Note the similarity of the phase tensor data for all the parameters, including the azimuth of the maximum of the phase tensors, despite the difference in the curves (Fig. 11). The phase tensor is independent of distortion and misalignment of the electric field array. The analysis of the derived distortion suggests that the electric field array was installed at an angle of 45° with respect to the magnetic field sensors.

REFERENCES

Bahr, K., 1988. Interpretation of the magnetotelluric tensor: regional induction and local telluric distortion, *J. Geophys.,* **62,** 119–127.

Bahr, K., 1991. Geological noise in magnetotelluric data: a classification of distortion types, *Phys. Earth planet. Inter.,* **66,** 24–38.

Bahr, K. & Simpson, F., 2002. Electrical anisotropy below slow- and fast-moving plates: paleoflow in the upper mantle?, *Science,* **295,** 1270–1272.

Berdichevsky, M.N., 1999. Marginal notes on magnetotellurics, *Surv. Geophys.,* **20,** 341–375.

Bibby, H.M., 1986. Analysis of multiple-source bipole-dipole resistivity surveys using the apparent resistivity tensor, *Geophysics,* **51,** 972–983.

Bibby, H.M. & Hohmann, G.W., 1993. Three dimensional interpretation of multiple source bipole dipole resistivity data using the apparent resistivity tensor, *Geophys. Prospect.,* **41,** 697–723.

Bibby, H.M., Caldwell, T.G. & Risk, G.F., 1998. Electrical resistivity image of the upper crust within the Taupo Volcanic Zone, New Zealand, *J. geophys. Res.,* **103,** 9665–9680.

Caldwell, T.G., Bibby, H.M. & Brown, C., 2004. The magnetotelluric phase tensor, *Geophys. J. Int.,* **158,** 457–469.

Chave, A.D. & Smith, J.T., 1994. On electric and magnetic galvanic distortion tensor decompositions, *J. geophys. Res.,* **99,** 4669–4682.

Egbert, G.D., 1990. Comments on 'Concerning dispersion relations for the magnetotelluric impedance tensor' by E. Yee and K.V. Paulson, *Geophys. J. Int.,* **102,** 1–8.

Groom, R.W. & Bailey, R.C., 1989. Decomposition of the magnetotelluric tensors in the presence of local three-dimensional galvanic distortion, *J. geophys. Res.,* **94,** 1913–1925.

Groom, R.W. & Bailey, R.C., 1991. Analytical investigations of the effects of near surface three-dimensional galvanic scatterers on MT tensor decomposition, *Geophysics,* **56,** 496–518.

Groom, R.W. & Bahr, K., 1992. Corrections for near surface effects: Decomposition of the magnetotelluric impedance tensor and scaling corrections for regional resistivities: A tutorial, *Surv. Geophys.,* **13,** 341–379.

Heise, W. & Pous, J., 2003. Anomalous phases exceeding 90° in magnetotellurics: anisotropic model studies and a field example, *Geophys. J. Int.,* **155,** 308–318.

Jiracek, G.R., 1990. Near-surface and topographic distortions in electromagnetic induction, *Surv. Geophys.,* **11,** 163–203.

Lazaeta, P. & Haak, V., 2003. Beyond magnetotelluric decomposition: Induction, current channelling, and magnetotelluric phases over 90°, *J. geophys. Res.,* **108**(B6), 2305, doi:10.1029/2001JB000990.

Lilley, F.E.M., 1998. Magnetotelluric tensor decomposition; Part I, theory for a basic procedure, *Geophysics,* **63,** 1885–1897.

McNeice, G.W. & Jones, A.G., 2001. Multisite, multifrequency tensor decomposition of magnetotelluric data, *Geophysics,* **66,** 158–173.

Ogawa, Y. et al, 1999. Magnetotelluric measurements across the Taupo Volcanic Zone, New Zealand—preliminary results, *Geophys. Res. Lett.,* **26,** 3673–3676.

Ogawa, Y. & Uchida, T., 1996. A two-dimensional magnetotelluric inversion assuming Gaussian static shift, *Geophys. J. Int.,* **126,** 69–76.

Ritter, P., 1996. Separation of local and regional information in geomagnetic response functions using hypothetical event analysis, *PhD thesis*, University of Edinburgh, Edinburgh.

Simpson, F., 2001. Resistance to mantle flow inferred from the electromagnetic strike of the Australian upper mantle, *Nature,* **412,** 632–635.

Singer, B.Sh., 1992. Correction for distortions of magnetotelluric fields: Limits of validity of the static approach, *Surv. Geophys.,* **13,** 309–340.

Smith, J.T., 1995. Understanding telluric distortion matrices, *Geophys. J. Int.,* **122,** 219–226.

Weaver, J.T., Agarwal, A.K. & Lilley, F.E.M., 2000. Characterization of the magnetotelluric tensor in terms of its invariants, *Geophys. J. Int.,* **141,** 321–336.

Weaver, J.T., Agarwal, T.A.K. & Lilley, F.E.M., 2003. The relationship between the magnetotelluric tensor invariants and the phase tensor of Caldwell, Bibby and Brown, in *Three-Dimensional Electromagnetics III Australian Society of Exploration*, Vol. 43, pp. 1–8, eds Macnae, J. & Liu, G., Geophysicists paper.

Zhang, P., Petersen, L.B., Mareschal, M. & Chouteau, M., 1993. Channeling contributions to tipper vectors: A magnetic equivalent to electric distortion, *Geophys. J. Int.,* **113,** 693–700.

APPENDIX: GRAPHICAL REPRESENTATION OF A TENSOR

The graphical representation of a second order second rank tensor is used in Bibby (1986) for the presentation of tensor dc resistivity data. This representation is outlined here in a slightly different form using, as the example, the distortion tensor **D**. The same technique can be used for any (real) second order tensor. The distortion tensor defines the relationship between the regional $\mathbf{E}_R$ and the measured **E** electric field vectors

$$\mathbf{E} = \mathbf{D}\,\mathbf{E_R}. \qquad (A1)$$

In effect the role of the distortion tensor **D** is to map the regional electric field vector into the measured vector. It is convenient to write the tensor in the form given in eq. (16), which uses the tensor invariants. That is, we write

$$\mathbf{D} = \mathbf{R}^{\mathrm{T}}(\alpha_D - \beta_D)\mathbf{G_D}\,\mathbf{R}(\alpha_D + \beta_D), \qquad (A2)$$

where $\mathbf{R}\,(\theta)$ is the rotation matrix, and $\mathbf{G}_D$ is a diagonal (gain) matrix given by

$$\mathbf{G_D} = \begin{bmatrix} D_{\max} & 0 \\ 0 & D_{\min} \end{bmatrix} \qquad (A3)$$

and angles α_D and β_D are defined in eq. (14). Note that β_D, $D_{\max}$ and $D_{\min}$ are invariants of **D**.

Now consider the effect of the distortion on a unit vector $\hat{\mathbf{E}}$ in direction θ. The corresponding measured electric field **E** is given by

$$\mathbf{E} = \mathbf{R}^{\mathrm{T}}(\alpha_D - \beta_D)\,\mathbf{G_D}\,\mathbf{R}(\alpha_D + \beta_D)\hat{\mathbf{E}}(\theta), \qquad (A4)$$

where

$$\hat{\mathbf{E}}(\theta) = \begin{bmatrix} \cos(\theta) \\ \sin(\theta) \end{bmatrix}.$$

As θ varies the vector **E** plots out an ellipse with major axis occurring when $\theta = (\alpha_D - \beta_D)$ (see Fig. 1). This is most easily shown by rotating the coordinate axes to the direction of the major axis. In the rotated coordinates

$$\begin{aligned} \mathbf{E}' &= \mathbf{R}(\alpha_D - \beta_D)\,\mathbf{E} \\ &= \mathbf{R}(\alpha_D - \beta_D)\,\mathbf{R}^{\mathrm{T}}(\alpha_D - \beta_D)\mathbf{G_D}\,\mathbf{R}(\alpha_D + \beta_D)\,\hat{\mathbf{E}}(\theta) \\ &= \mathbf{G_D}\,\mathbf{R}(\alpha_D + \beta_D)\,\hat{\mathbf{E}}(\theta). \end{aligned} \qquad (A5)$$

Writing $\mathbf{E}'$ in component form

$$\begin{bmatrix} E'_x \\ E'_y \end{bmatrix} = \mathbf{G_D} \begin{bmatrix} \cos(\theta - \alpha_D - \beta_D) \\ \sin(\theta - \alpha_D - \beta_D) \end{bmatrix}. \qquad (A6)$$

Using the definition of $\mathbf{G}_D$

$$\begin{bmatrix} E'_x \\ E'_y \end{bmatrix} = \begin{bmatrix} D_{\max}\cos(\theta - \alpha_D - \beta_D) \\ D_{\min}\sin(\theta - \alpha_D - \beta_D) \end{bmatrix}, \qquad (A7)$$

which is the parametric equation for an ellipse with semi-major and semi-minor axes of length $D_{\max}$ and $D_{\min}$, respectively. Eliminating $(\theta - \alpha_D - \beta_D)$ gives the equation for the ellipse:

$$E_x'^{\,2}/(D_{\max})^2 + E_y'^{\,2}/(D_{\min})^2 = 1. \qquad (A8)$$

Relative to the original axes, the principal axis of the ellipse occurs when **E** is in the direction $(\alpha_D - \beta_D)$. However, this occurs when $\hat{\mathbf{E}}(\theta)$ is in the direction θ where

$$\theta = \alpha_D + \beta_D. \qquad (A9)$$

Thus, the effect of the distortion tensor is to rotate the electric field vector by $2\beta_D$.

An example of the elliptical representation of the phase tensor **Φ** is shown in Fig. 1. The principal axes (shown as $\Phi_{\max}$ and $\Phi_{\min}$) together with the angle β are rotational invariants although α is not. The angle $\alpha - \beta$ defines the orientation of the semi-major axis of the ellipse (Fig. 1) relative to the coordinate axes. The angle α is the principal axis of the symmetric part of **D** and defines a reference axis, which lies at an angle β relative to the major axis of the ellipse. Rotations of the coordinate axes will change only the angle α so that the ellipse and the reference axis can be thought of as fixed relative to the Earth. The angle α thus defines the orientation of the ellipse and its reference axis relative to the coordinate axes, or equivalently, defines the coordinate axes relative to the ellipse.

Note that when the real and imaginary components of the MT impedance tensor are plotted using this technique the angle β is not near zero as it is for a diagonally dominant tensor such as the phase tensor. In uniform conditions the magnetic and electric field vectors are orthogonal. Thus the impedance tensor, which is a mapping of the magnetic field onto the electric field, must include a rotation of the magnetic vector by about 90°. This is accommodated by a value of 2β of approximately 90° ($\beta \approx 45$).